SUPPLEMENT MATERIAL

Chemoreceptor hypersensitivity, sympathetic excitation, and overexpression of ASIC and TASK channels prior to hypertension in SHR

This online supplement includes:

Materials and Methods

Male SHR and WKY rats (ages 4-6 weeks) were used in these experiments. At that age, the SHR are prehypertensive (1-4); their blood pressure begins to increase progressively after 6-8 weeks and exceeds values in WKY rats reaching a maximal sustained level after approximately 15 weeks (Online Figure I).

Isolation of carotid bodies

Rats were deeply anesthetized by isoflurane inhalation and decapitated. The carotid bifurcation was exposed and both carotid bodies removed. Carotid bodies (CB) were placed in ice cold PBS until preparation for PCR and in ice cold Hibernate A (Braintree) prior to glomus cell isolation for electrophysiologic studies. The project had been approved by the University of Iowa Animal Care and Use Committee.

Culture of carotid body glomus cells

Established protocols describing the isolation of glomus cells from rat carotid bodies were followed (S5, 6). Two carotid bodies were excised from each of 54 SHR and 71 WKY rats, 4-6 weeks of age. The isolated carotid bodies were incubated in 1 cc of nominally Ca^{2+} - and Mg^{2+} -free Tyrode solution containing collagenase (2 mg ml^{-1}; Type IV; Worthington), trypsin (0.4 $mgml^{-1}$; Worthington) and deoxyribonuclease (DNase II, 0.5 $mgml^{-1}$; Worthington) at pH 7.4 for 31 minutes at 37°C. At 25 and 31 minutes the carotid bodies were mechanically disrupted for 1 minute by repeated aspiration through a fire polished Pasteur pipette treated with Aquasil Siliconizing Fluid (Pierce). Digestion was terminated at 31 minutes by dilution of the enzymes with 3 ml of a DMEM/0.1% BSA solution and cells were pelleted (2000 RPM for 8 minutes). The supernatant was discarded, the cells resuspended in 2 ml of the same solution and centrifuged for 5 minutes again. After discarding the supernatant the pellet was finally resuspended in 200 µl (400 µl for 2 rats) of culture medium (F-12/DMEM (1:1) plus, 5% fetal calf serum supplemented with 10,000 U/ml Pen V/Streptomycin and 10mM HEPES. 100 µl aliquots were plated onto

small poly-D-lysine-coated coverslips placed in 35 mm Petri dishes and incubated at 37° C with an atmosphere of 5% CO2 in air. Two hours later, when the cells are attached, 2 ml of culture medium was added to the Petri Dish. Spherical glomus cells ranging in size from 7 to 12 μm in diameter and without processes were chosen for recording 2-8 hours after plating.

Perforated patch clamp recording

Coverslips were transferred into a 1.0 ml recording chamber on the stage of an inverted microscope (Nikon). Whole-cell patch clamping was performed as described previously (S5) except that the perforated whole-cell mode was used in this study to maintain the integrity of the intracellular milleu. Membrane current or membrane potential were recorded with an Axopatch 200A amplifier (Axon Instruments, CA) interfaced with a personal computer. Cells with a resting membrane potential positive to -40 mV were discarded. All the cells accepted in this study had significant voltage-gated outward currents. Voltage was held at -60 mV to record ASIC currents. The patch pipettes (4 - 7 MΩ) were pulled from borosilicate glass (BF100-50-10, Sutter instrument, CA). The pipette solution consisted of (mmol/L): 35 KCl, 57.5 K_2SO_4, 2 $MgCl_2$, 1 Na_2ATP, 10 EGTA, 20 HEPES with pH adjusted to 7.2 by KOH. Amphotericin B at a final concentration of 240 μg/mL was used for membrane perforation. Recordings were filtered at 5 kHz and digitized at 10-50 kHz using a Digidata 1200 interface (Axon Instruments, CA), and pCLAMP9.0 (Axon Instruments, CA) was used for data acquisition and data analysis. Low pH – induced inward currents and membrane depolarizations were filtered at 1 kHz using Clampfit. The ramp currents were filtered at 50 Hz. To test the effects of extracellular acidosis on glomus cells, we used brief applications of acidic solutions while maintaining a high intracellular buffering capacity using HEPES to prevent intracellular pH changes (5). Solutions of varying pH were delivered topically to patch-clamped cells through a pipette (500 μm in diameter) using a valve controller (VC-6, Warner Instrument Corp). Fast exchange of the varying pH solutions was achieved within 20 ms and tested by measuring a change in the liquid-junction potential between the recording pipette and bath solutions. The standard bath solution contained (mmol/L): 140 NaCl, 5 KCl, 2 $CaCl_2$, 2 $MgCl_2$, 20 HEPES, 5 Dextrose, pH was adjusted to 7.4 by NaOH. Acidic solutions from pH 5.5 to pH 7.0 were buffered using a combination of 10 mmol/L HEPES and 10 mmol/L MES. For TASK current recordings, the bath solution contained (mmol/L): 140 NaCl, 5 KCl, 2 $MgCl_2$, 20 HEPES, 5 Dextrose, 0.5 EGTA, pH was adjusted to 7.4 by NaOH. Acidic solutions from pH 8.0 to pH 6.0 were buffered using a combination of 10 mmol/L HEPES and 10 mmol/L 2-(N-morpholino) ethanesulfonic acid.

Data analysis

Data are expressed as means ± SEM. pH dose–response curves were fit to sigmoidal dose–response functions using the following Hill equation: $Y = Y_0+A/ (1 + ([H^+]_{50}/X)^b)$, where X is the concentration of proton and Y is the response. The H+ concentration causing half maximal activation is presented as $[H^+]_{50}$. pH_{50} was then calculated from $[H^+]_{50}$. Statistical differences were analyzed by Student's t test, Chi Square or ANOVA. Significance was set at $p<0.05$.

Real-time RT PCR.

Measurements were made on tissue from 1 month old rats. Carotid bodies were removed as described above. Total RNA was extracted from the two carotid bodies of each of five SHR and each of five WKY rats by using Trizol reagent (Invitrogen), and reversely transcribed into cDNA by using AffinityScriptTM QPCR cDNA Synthesis Kit (Stratagene) according to the manufacturer. The quantitative PCR was carried out by using Model 7000 real-time PCR system (ABI), Brilliant SYBR Green QPCR Master Mix (Stratagene) and gene specific primers

according to the protocol provided by the manufacturer. The primers were designed in the lab, and their sequences are given in Online Table I. The oligomers were purchased from Integrated DNA Technologies (IDT, IA). The expression of GAPDH (Glyceraldehyde-3-phosphate dehydrogenase) was used to normalize the measurements.

Online Table I. PCR primer sequences

Target Gene Fragment	Genbank Accession	Primer Sequences
TASK1 62 bp	AF031384	Forward: 5′-CTT CGC CGG CTC CTT CTA CT-3′
		Reverse: 5′-CCG CAT GAC CAT AGC CGA TT-3′
TASK3 112 bp	AF192366	Forward: 5′-AGC TGG TAA TCC TGC AGT CT-3′
		Reverse: 5′-GCA GCA TGT CCA TAT CCG ATAG-3′
ASIC1b 80-bp	AJ006519	Forward: 5′-GCT GGA GGA CAT GCT GCT CTA T-3′
		Reverse: 5′-ACC GAG TGA AGA CCA CTG AGA A-3′
ASIC3 163-bp	NM_173135	Forward: 5′-TGT CAG CAG CAG CAA CTG AG-3′
		Reverse: 5′-AGG CCA GGC GAC AAC-CTA-TT-3′
GAPDH 119 bp	NM_017008	Forward: 5′-CTG CAC CAC CAA CTG CTT AG-3′
		Reverse: 5′-GGC CAT CCA CAG TCT TCT GA-3′

Western blotting.

Eight carotid bodies were pooled from four WKY rats and eight were pooled from four SHR at 1 month of age. They were washed twice with PBS, and homogenized in lysis buffer: 50 mmol/L Tris-HCL, 0.1% sodium dodecyl sulphate (SDS), 100 μg/mL phenyl methyl sulphonal fluoride, 150 mmol/L NaCl, pH 8.0) plus 1% Triton X-100, 3X Halt Protease Inhibitor Cocktail and 1X EDTA (Pierce). The lysates were then vortexed, and sonicated on ice with three bursts of 20 s ultrasonic irradiation (Microson Ultrasonic Cell Disruptor). A membrane protein extraction kit (Pierce) was used to extract the cellular membrane proteins. The total cellular protein concentration was determined by using a Bio-Rad Protein Assay kit (Bio-Rad). Protein (60 μg) was denatured with an equal volume of 2X gel SDS loading buffer at 95^{o}C for 5 min, and run on a SDS-7.5% Tris-HCl polyacrylamide gel for 1 hr at 170 volts in Biorad Cell with DS-Tris-glycine running buffer. The proteins in gel were equilibrated in 20% methanol transfer buffer and then transferred electrophoretically to a nitrocellulose membrane at 100 volts for 75 min. Membrane was blocked with 5% (wt/vol) nonfat milk in Tween-Tris-buffered saline (TTBS: 0.02 M Tris and 0.15 M NaCl buffer, containing 0.1% Tween 20, pH 7.45) for one hour at room temperature. The antibodies used are listed in Online Table II. The membrane was then incubated in 1:200 antibody TTBS buffer of the anti-TASK1, ASIC1 and ASIC3 antibodies overnight, and then for one hour at room temperature with horseradish peroxidase- conjugated secondary IgG antibodies matched to the hosts, primary antibodies. For example, for the primary antibody goat anti-ASIC1, we used the secondary antibody donkey anti-goat IgG HRP; and for rabbit anti-ASIC3, used mouse anti-rabbit IgG HRP. The antibody activities were detected with an enhanced chemiluminescence detection system (Pierce Chemical) and exposure to X-ray film. After this step, the membrane was stripped and reprobed with anti-β-actin antibody for the purpose of normalizing protein loading according to the density of the β-actin band. The protein standard marker (BenchMark Pre-Stained Protein Ladder, Invitrogen) was used to evaluate the transfer efficiency and to locate the ranges of protein molecular weights after electrophoresis. The bands

taken for analysis were ASIC1 (~ 60kDa), ASIC3 (~ 60 kDa), TASK1 (50 ~ 65 kDa) and β-actin (~ 42 kDa). The densities of the bands were analyzed by using software ImageJ 1.40g. Similar Western blot analyses were carried out on brain tissue from WKY and SHR for contrasting brain to carotid body expression.

Online Table II. Antibodies used in this study

Antibody	Maker & Cat #	Application	
Primary ab		WB	IF
Goat anti-ASIC1	Santa Cruz, sc-16009	1:500	-
Mouse anti-TH	Santa Cruz, sc-25269	-	1:50
Goat anti-TASK1	Santa Cruz, sc-11309	1:500	1:50
Rabbit anti-ASIC3	Abcam, ab49333	1:500	1:10
Mouse anti-β-actin	Sigma, A5441	1:2000	-
Secondary ab			
Donkey anti-goat IgG HRP	Santa Cruz, sc-2020	1:10000	
Mouse anti-rabbit IgG HRP	Santa Cruz, sc-2357	1:10000	
Goat anti-mouse IgG HRP	Santa Cruz, sc-2005	1:10000	
Donkey anti-mouse IgG TEAS RED	Santa Cruz, sc-2098	-	1:200
Donkey anti-goat IgG TEXAS RED	Santa Cruz, sc-2783	-	1:200
Donkey anti-goat IgG FITC	Santa Cruz, sc-2024	-	1:200
Mouse anti-rabbit IgG FITC	Santa Cruz, sc-53806	-	1:200

Immunohistochemistry of glomus cells in clusters

The methods for isolation and culture of glomus cells in clusters were as described above except for a shorter period of trituration to reduce the dispersion of individual cells.

Clusters of glomus cells in culture for 20 hours were fixed with ice-cold fixative, 4% paraformaldehyde in phosphate buffered saline (PBS, GIBCO). Slides were subjected to a staining procedure of double-antibodies labeling for immunochemical analysis using a confocal microcope (Bio-Rad 1024).

After washing with PBS plus 0.1% Tween 20, the slides were blocked in solution containing 3% BSA (Bovine Serum Albumin) plus 0.5% Triton X-100 in PBS for 1 hour, and then incubated for 16-18 hours at 4^{o}C with primary antibodies in block solution (1:10 or 1:50). After rinsing three times for 5 minutes in PBS, slides were incubated for 1 hour with secondary antibodies diluted 1:200 in blocking solution.

Primary antibodies used were anti-enzyme tyrosine hydroxylase (anti-TH), anti-TASK1 purchased from Santa Cruz, and anti-ASIC3 from Abcam as listed in Online Table II. Fluorescent stain was obtained by using fluorescein (green) or Texas Red (red) conjugated secondary antibodies matched to the hosts' primary antibodies (for example, we used the secondary antibody mouse anti-rabbit IgG FITC for the primary antibody rabbit anti-ASIC3; and donkey anti-mouse IgG TEAS RED for mouse anti-TH). Preparations without the primary antibody were used for controls. Sample slides were washed 3 times using PBS (5 min each) and a drop of Vectashield Mounting Medium (Vector Laboratories, Burlington, Ontario, Canada) was added before applying the coverslip. The samples were viewed using the Bio-Rad 1024 Laser Scanning

Confocal Microscope, equipped with the lasers of Argon (488 and 514 nm) and helium-neon (543 nm).

Hemodynamic, autonomic and ventilatory responses to peripheral chemoreceptors stimulation in prehypertensive SHR and normotensive WKY.

The working heart-brainstem preparation was used as described previously (4, 7). Rats (SHR and WKY, 4-5 weeks old) were anesthetized with isoflurane and decerebrated. They were bisected sub-diaphragmatically and exsanguinated and anesthesia withdrawn. The head and thorax was placed in ice-chilled Ringer's (composition in mM: 125 NaCl, 24 $NaHCO_3$, 5 KCl, 2.5 $CaCl_2$, 1.25 $MgSO_4$ and 1.25 KH_2PO_4, 10 dextrose, pH 7.4 after carbogenation (5% CO_2, 95% O_2)). The descending aorta was isolated and retrograde perfusion of the thorax and head was achieved via a double-lumen catheter (1.25mm, DLR-4, Braintree Scientific, MA, USA) inserted into the descending aorta. The perfusate was the Ringer's solution (see above) containing Ficoll (1.25%) warmed to 31°C and gassed with carbogen. The second lumen of the cannula was connected to a transducer to monitor perfusion pressure in the aorta. Flow was adjusted until an augmenting (i.e. eupneic) pattern of phrenic nerve activity (PNA) was achieved (15-19 $mL.min^{-1}$ gave 45-70 mmHg). Neuromuscular blockade was established using vecuronium bromide added to the perfusate (4 $\mu g.ml^{-1}$, Organon Teknica, Cambridge, UK). Simultaneous recordings of PNA and thoracic sympathetic nerve activity (tSNA, T8-T10) were obtained using glass suction electrodes, amplified (20kHz, Neurolog), filtered (50-1500kHz, Neurolog), digitized (CED, Cambridge, UK) and recorded to hard disk using Spike 2 (CED). Heart rate was derived from the R-wave of the electrocardiogram (ECG) recorded simultaneously with the phrenic nerve activity. The peripheral chemoreceptors were stimulated using sodium cyanide (NaCN; 0.05% solution; 100 µl bolus) injected into the aorta or carotid arteries. The increase in central respiratory rate, maximum bradycardia and the percentage increase in tSNA were all analyzed. tSNA was rectified and integrated with a time constant of 100ms and the noise level subtracted as assessed after applying xylocaine (0.5%) to the sympathetic chain at the end of each experiment. Reflexly evoked sympathetic nerve discharge was averaged separately during the phrenic burst and the inter-phrenic interval (3 bursts/intervals in control and during the response) as previously described (4, 7).

Data analysis.

Data are expressed as means ± SEM. Statistical differences were analyzed by unpaired Student's *t* test, Chi Square or ANOVA. Posthoc test with a Bonferroni correction was further used. Significance was set at $P<0.05$.

Results

Effect of amiloride on the rapid inward current (Online Figure II).

Representative tracings and group data shown in Online Figure II indicate a greater rapid inward current in SHR than in WKY at pH 6.0 and its blockade with essentially a complete recovery after amiloride.

Effects of amiloride and quinidine on the acid-induced depolarizations (Online Table III).

Figure 5 in the main text shows individual tracings of the initial rapid and sustained depolarizations in 4 cells: 2 from WKY and 2 from SHR. They portray the selective inhibition of the initial depolarizations by amiloride and the selective inhibition of the sustained

depolarizations by quinidine. The Online Table III shows the mean ± SE of the group data which confirm the effectiveness and selectivity of the blockers and indicate that full recovery of the responses was achieved.

Online Table III: Selective effects of Amiloride and Quinidine on initial and sustained depolarizations in response to low pH

		Initial depolarization (ΔmV)			Sustained depolarization (ΔmV)		
	Number	Control	**Amiloride**	Recovery	Control	**Amiloride**	Recovery
WKY	6	15.7±2.9	2.0±1.0†	16.2±4.7	30.0±3.0	29.8±3.3	31.0±3.1
SHR	6	24.2±4.7	2.7±1.0†	25.3±5.7	36.8±2.1	37.3±3.5	39.7±2.3
		Control	**Quinidine**	Recovery	Control	**Quinidine**	Recovery
WKY	5	13.8±4.6	17.5±4.9	13.0±6.2	23.3±5.0	12.4±2.5*	21.3±2.3
SHR	5	20.4±6.7	21.6±9.5	17.8±6.9	37.0±4.0	16.8±2.2*	29.8±4.4

Responses (ΔmV) to low pH 6.0 in WKY vs. SHR glomus cells. Values are means±SEM. Amiloride selectively and significantly inhibited the initial depolarization (†P<0.01) in both WKY and SHR glomus cells. Conversely, quinidine selectively and significantly inhibited the sustained depolarizations (*P<0.05).

Effect of low pH on voltage-gated channels in glomus cells (Online Fig. III).

We have shown (*Circ. Res.* 2007) that low pH depolarizes glomus cells predominantly by altering conductances of two non-voltage-gated channels. ASIC channels are activated while TASK channels are inhibited resulting in rapid early depolarization followed by sustained depolarization respectively. In this study we report that these responses are enhanced in prehypertensive SHR. Following pharmacologic blockade of these two channels with amiloride and quinidine the majority of the pH-induced depolarization is abrogated.

To further test the effect of pH on voltage gated currents in glomus cells we used patch clamp recordings of currents induced by a slow ramp depolarization from -100 mV to 0 mV over a period of two seconds. An exponential increase in outward current was noted when the cells were almost fully depolarized between -30 and 0 mV. This large current was reversibly inhibited by both low pH and quinidine (Online Fig. IIIA).

Moreover, when we applied rapid incremental step depolarizations of 50 msec. duration from a holding potential of -60 to -40 mV and then progressively up to +20 mV large outer currents were induced. These currents were increased by raising pH from 7.4 to 8.0 and then reduced by stepwise lowering of pH from 8.0 to 6.0. The partial blockade of these currents was reversed when pH was restored from 6.0 to 7.4 (Online Fig. IIIB). The magnitude of inhibition of these currents by lowering pH from 8.0 to 6.0 was comparable in SHR and WKY glomus cells (Online Fig. IIIC). We question the functional relevance of these currents since glomus cells rarely develop action potentials and these outward currents are largest when the cells are markedly depolarized or at a positive membrane potentials.

Effects of intraarterial NaCN in SHR and WKY Rats (Online Table IV).

Stimulation of peripheral chemoreceptors with intraarterial cyanide caused increases in tSNA, in perfusion pressure, and in central respiratory drive (frequency of phrenic nerve activity bursts) and decreases in heart rate. These are portrayed in Figure 8A in the main text, which contrasts responses in an SHR and a WKY rat. The online Table IV shows the mean ±SE of the group data. Ventilatory, autonomic, and hemodynamic responses to NaCN were not statistically different in SHR vs. WKY rats with the exception of the increase in tSNA, which was significantly greater in SHR during expiration and the bradycardia, which was less pronounced in SHR.

Online Table IV. Responses to chemoreceptor stimulation with NaCN in SHR vs. WKY

	HR (Δbeats/min.)	PP (ΔmmHg)	tSNA (Insp.) (%Δ)	tSNA (Expir.) (%Δ)
WKY	-286 ±21.9	9.0 ±0.89	109 ±29.1	78.5 ±16.8
SHR	-197* ±23.2	7.3 ±1.3	102 ±25.9	237*# ±37.5

Phrenic Nerve Activity

	Baseline				
	Frequency (bursts/min)	Insp. Length (s)	Expir. Length (s)	% Δ freq. (Δ interburst interval)	% Δ in amplitude
WKY	19.9 ±1.9	0.69 ±0.06	2.7 ±0.34	111 ±28.7	9.7 ±2.7
SHR	17.5 ±0.97	0.79 ±0.06	2.8 ±0.25	96.9 ±20.8	11.7 ±2.2

Δ indicates the response to NaCN; HR = heart rate; PP = perfusion pressure; tSNA = thoracic sympathetic nerve activity; Insp. = inspiration; Expir. = expiration; s = seconds; freq. = frequency. * = $P<0.05$ for WKY vs. SHR; # = $P<0.01$ for expiration vs. inspiration in SHR.

References

1. Andresen MC, Kuraoka S, Brown AM. Baroreceptor function and changes in strain sensitivity in normotensive and spontaneously hypertensive rats. *Circ Res*. 1980;47:821–828.
2. Cabassi A, Vinci S, Calzolari M, Bruschi G, Borghetti A. Regional sympathetic activity in pre-hypertensive phase of spontaneously hypertensive rats. *Life Sci*. 1998;62:1111–1118.
3. Korner P, Bobik A, Oddie C, Friberg P. Sympathoadrenal system is critical for structural changes in genetic hypertension. *Hypertension*. 1993;22:243–252.
4. Simms AE, Paton JFR, Pickering AI, Allen AM. Amplified respiratory-sympathetic coupling in the spontaneously hypertensive rat: does it contribute to hypertension? *J Physiol*. 2009;587:597–610.
5. Tan ZY, Lu Y, Whiteas CA, Benson CJ, Chapleau MW, Abboud FM. Acid-sensing ion channels contribute to transduction of extracellular acidosis in rat carotid body glomus cells. *Circ Res*. 2007;101:1009–1019.
6. Lopez-Lopez JR, Gonzalez C, Perez-Garcia MT. Properties of ionic currents from isolated adult rat carotid body chemoreceptor cells: effect on hypoxia. *J Physiol*. 1997;499:429–441.
7. Paton JFR. A working heart-brainstem preparation of the mouse. *J Neurosci Meth*. 1996;65:63–68.

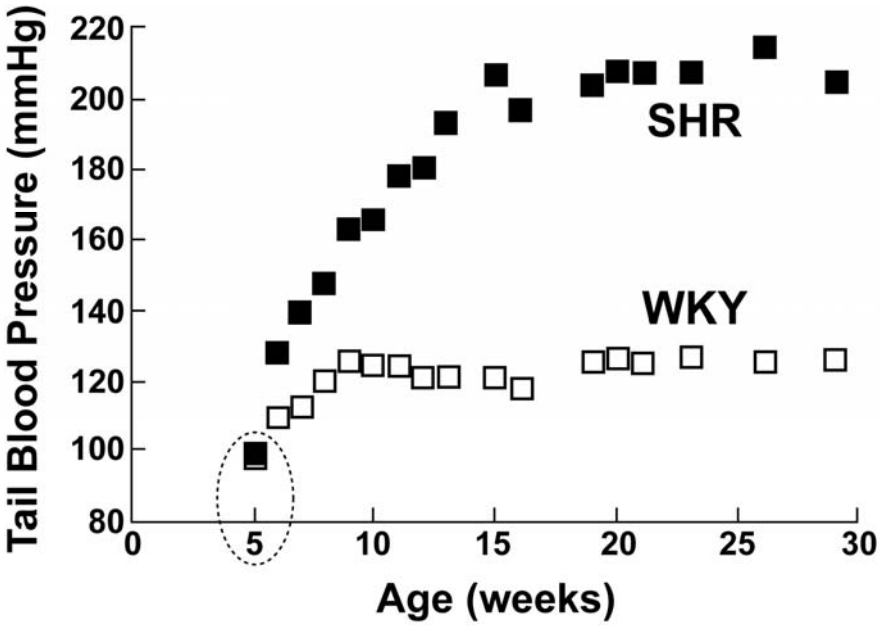

Online Figure I: Age-dependent increases in blood pressure in SHR and WKY. (Adapted from ref. #1 Andresen et. al, Circ. Res. 1980;47:821-828.)
Values are means of systolic pressure from 10–30 rats each and the SE were smaller than the symbols. At 6 weeks SHR had a pressure that was still equivalent to that of the normotensive adult WKY. Before 6 weeks of age blood pressure in SHR was not significantly different than that in WKY and considered to be in the prehypertensive phase.

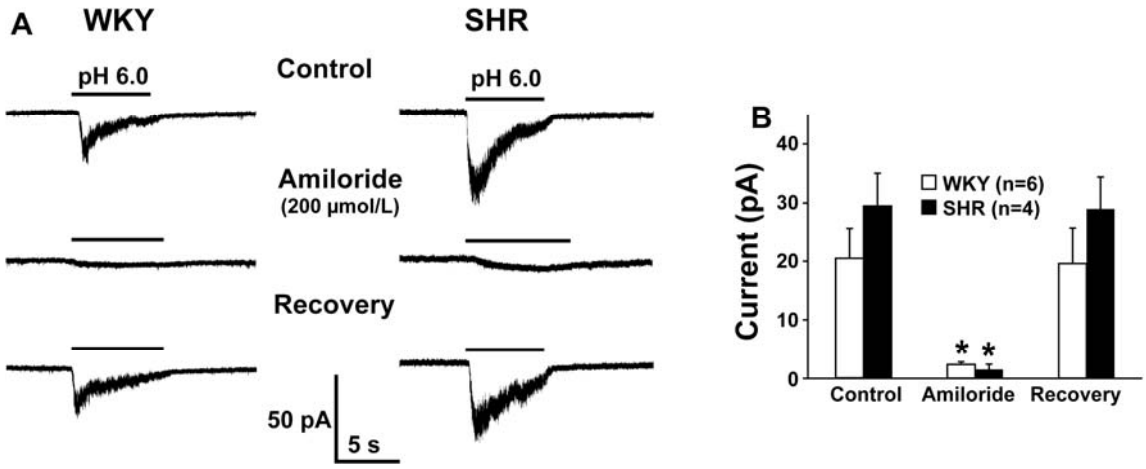

Online Figure II: Amiloride blocks rapid inward current evoked by extracellular acidosis in glomus cells from WKY rats and SHRs.
A) Representative currents from a WKY and a SHR glomus cell show inhibition of inward current by pH 6.0 and recovery. A residual small sustained inward current was noted at low pH after amiloride;
B) Mean maximum current ± SE from WKY and SHR glomus cells show inhibition and recovery of the rapid inward current
(* $P<0.05$ for amiloride vs. control and recovery).

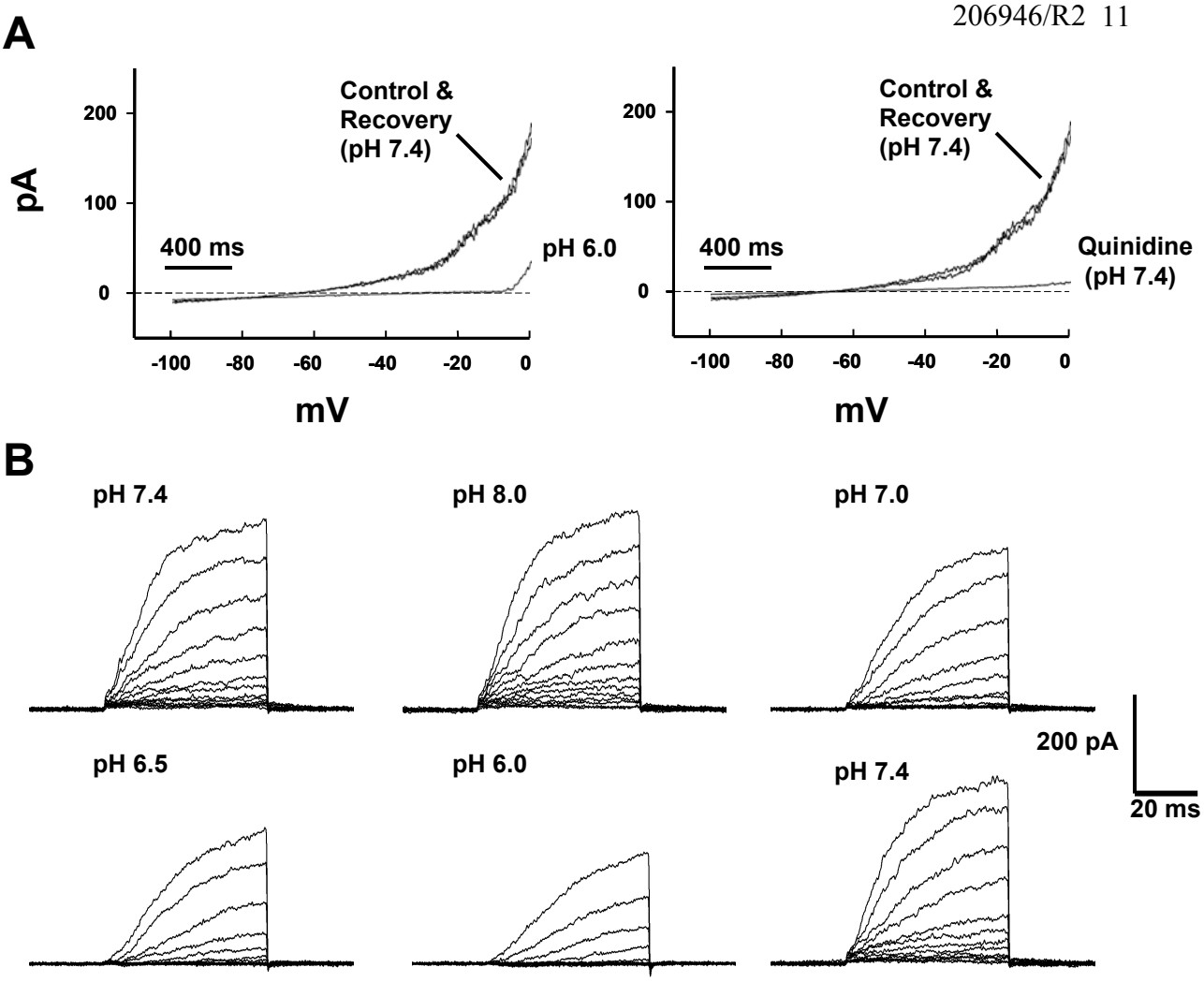

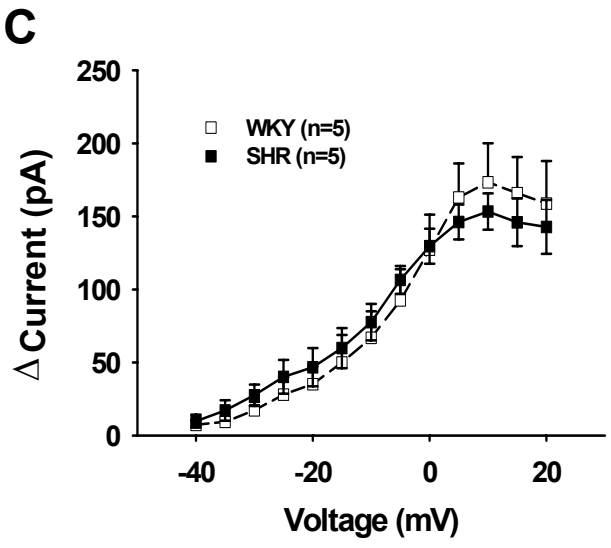

Online Figure III: A) Effect of low pH (6.0) and quinidine on the outward current induced by a slow ramp depolarization over a 2 second period from -100 mV to 0 mV. An exponential increase in pH and quinidine-sensitive currents occurs with pronounced depolarization; **B)** Effect of pH on voltage-gated outward currents evoked by incremental depolarizing pulses of 50ms duration from a holding potential of -60 to -40 mV and then progressively up to +20 mV in 5 mV increments. The currents increased with pH 8.0, then declined with low pH, and recovered at pH 7.4; **C)** pH 6.0-induced reduction of voltage-gated outward currents seen during step depolarizing pulses from -60 to -40 mV and then progressively to +20 mV. Values are mean ±SE of the magnitude of decline in outward currents from levels obtained at pH 8.0 to levels at pH 6.0 (ΔpA). The values increased progressively with greater depolarizations reaching a plateau at about +10 mV. There were no significant differences between SHR and WKY.